The ENSO Effect on World Wheat Market Dynamics: Smooth Transitions in Asymmetric Price Transmission

David Ubilava

Lecturer in the School of Economics at the University of Sydney
david.ubilava@sydney.edu.au

Selected Paper prepared for presentation at the Agricultural & Applied Economics Association's 2014 AAEA Annual Meeting, Minneapolis, MN, July 27-29, 2014.

The ENSO Effect on World Wheat Market Dynamics: Smooth Transitions in Asymmetric Price Transmission

Abstract

Climate anomalies, such as El Niño Southern Oscillation (ENSO), affect agricultural production in different parts of the world, and can impact price behavior of the internationally traded commodities. This study examines the effect of ENSO on wheat price dynamics of five major exporting regions – USA, Canada, Australia, EU, and Argentina. While the prices are linked due to the law of one price and the arbitrage conditions, nonlinear price adjustments are expected, due to the transaction costs, the market power, derived asymmetries from supply shocks. This study addresses asymmetries in wheat price transmission in response to ENSO-related supply shocks, using univariate and multivariate smooth transition modelling frameworks. Results of this study confirm regime-dependent nonlinearities in ENSO cycles as well as the system of considered wheat prices, where regimes are conditioned on the state of nature of the ENSO anomaly. In general, positive ENSO shocks, i.e. El Niño-s, result in wheat price reduction, while negative ENSO shock, i.e. La Niña-s, results in increased wheat prices. Moreover, the asymmetric nature of the responses to ENSO shocks implies that the rates of price increases are, on average, larger as compared to the rates of price decreases.

Keywords: Asymmetric Cycles; El Niño Southern Oscillation; Smooth Transition Modelling; Wheat Price Dynamics.

1 Introduction

The 2012 U.S. drought of historic magnitudes, followed by the record-setting temperatures in Australia, heated up the discussion about climate change and its economic consequences. In this context there has been growing interest in the role of climate change on climate anomalies, and, in turn, the effect of climate anomalies on economic performance. For example, a prolonged La Niña phase (of the El Niño Southern Oscillation cycle) has been cited as the potential common source of the aforementioned weather extremes (e.g. Mallya et al., 2013). Climate change and climate anomalies are not mutually exclusive, and, moreover, studies have suggested that climate change may result in more frequent and amplified climate anomalies (e.g. Rosenzweig et al., 2001). Nonetheless, the causes and consequences of climate change are beyond the scope of this research. Instead, this study primarily focuses on climate anomalies – the quasi-periodic climate patterns – and their economic consequences. In particular, this research examines asymmetric cycles of the El Niño Southern Oscillation (ENSO), and its effects on world wheat price dynamics.

Climate anomalies conceptually differ from climate change in that they tend to follow some cyclical pattern, and the cycles repeat every several years. That is, whether or not the climate is changing, the anomalies revolve around some long-run mean within the given climate reality. Thus, when the cycle is near its long-run mean, conditions are known as *normal* or *neutral*. Deviations from the neutral conditions are called *anomalies*. In the case of ENSO, the two extreme anomalies are *El Niño*, which denotes a positive deviation and is associated with warming sea-surface temperatures in the equatorial Pacific, and *La Niña* – the counterpart of El Niño. El Niño and La Niña can impact and amplify weather conditions in different parts of the world, causing severe damages to production and infrastructure (e.g. Ropelewski and Halpert, 1987; Rosenzweig et al., 2001). Moreover, the impact is not necessarily symmetric, i.e. weather conditions in some regions may be correlated with ENSO during one of it's phases, but not during the other. The asymmetries, in turn, offer additional intricacies to the already peculiar nature of the ENSO effect on world agricultural production and prices. This study unveils some of these peculiarities in relation to wheat production and prices.

The international wheat market is characterized by a small number of major exporting countries. This implies the possibility of exercising market power by exporters, but also makes the market susceptible to systemic weather shocks. Thus far, studies have assessed the oligopolistic behavior of wheat exporters, the spatial arbitrage opportunities, and the law of one price hypotheses (e.g. Goodwin and Schroeder, 1991; Mohanty et al., 1995, 1999; Bessler et al., 2003). Less has been done to investigate the impact of climate anomalies on international wheat price dynamics. This research aims to fill the aforementioned gap in the literature.

There is, at least, anecdotal evidence suggesting causal links between ENSO shocks and unfavorable weather conditions in major wheat-producing countries. Because of a relatively high concentration, both in terms of the number of major producers as well as their geographic distribution, the ENSO effect on wheat price dynamics becomes simply an economic corollary. This research examines the (possibly nonlinear) relationship between the ENSO anomalies and the vector of wheat prices from major exporting regions.

There are a number of reasons to believe that the horizontal price transmission in global wheat markets, as well as the effect of ENSO cycles on this relationship, can be nonlinear. Firstly, commodity price cycles reveal nonlinearities in terms of their magnitude and duration (Cashin et al., 2002). Moreover, while the international prices of homogeneous commodities are closely linked due to trade and arbitrage activities (Goodwin and Schroeder, 1991), transaction costs may mitigate their co-movement within the so-called "neutral band" (Goodwin and Piggott, 2001). Because of the perceived nonlinearities, adequate modelling techniques should be applied to properly examine wheat price dynamics.

This research adopts a vector smooth transition autoregression (VSTAR)[1] to address regime-dependent asymmetries in ENSO and wheat price dynamics (e.g. Rothman et al., 2001). The VSTAR is a multivariate extension of the smooth transition autoregression (Teräsvirta, 1994; van

[1] Alternatively and equivalently referred as the smooth transition vector autoregression (STVAR).

Dijk et al., 2002), which, in turn, is a generalization of the threshold autoregression (Tong and Lim, 1980; Tong, 1990). Some of the dynamic properties of these models, including specification and diagnostics, are explored in the estimation stage of the analysis. Additionally, this study adopts simulation methods, in particular, the generalized impulse response functions of Koop et al. (1996) to illustrate asymmetries in ENSO and wheat price cycles in response to the ENSO anomalies.

In what follows, we will briefly describe the modelling and testing frameworks of smooth transition models. We will then introduce the data used in this research. In the results section we will present estimated models, and highlight the advantages of nonlinear modelling. We will further illustrate the results via generalized impulse-response analysis. Finally, we will conclude this research by highlighting its main findings.

2 The Econometric Model and Linearity Tests

Let $\boldsymbol{x}_t = (\boldsymbol{y}_t', z_t)'$, where $\boldsymbol{y}_t = (y_{1,t}, y_{2,t}, \ldots, y_{n-1,t})'$ is a vector of endogenous variables, and z_t is weakly exogenous to $\boldsymbol{y}_t$. Then the relationship between z_t and $\boldsymbol{y}_t$ can be given by vector autoregression:

$$\boldsymbol{x}_t = \boldsymbol{\alpha} + \sum_{i=1}^{p} B_i \boldsymbol{x}_{t-i} + \boldsymbol{\varepsilon}_t, \tag{1}$$

where

$$B_i = \begin{bmatrix} \beta_{y_1,i}^{y_1} & \beta_{y_1,i}^{y_2} & \cdots & \beta_{y_1,i}^{y_{n-1}} & \beta_{y_1,i}^{z} \\ \beta_{y_2,i}^{y_1} & \beta_{y_2,i}^{y_2} & \cdots & \beta_{y_2,i}^{y_{n-1}} & \beta_{y_2,i}^{z} \\ \vdots & \vdots & \ddots & \vdots & \vdots \\ \beta_{y_{n-1},i}^{y_1} & \beta_{y_{n-1},i}^{y_2} & \cdots & \beta_{y_{n-1},i}^{y_{n-1}} & \beta_{y_{n-1},i}^{z} \\ 0 & 0 & \cdots & 0 & \beta_{z,i}^{z} \end{bmatrix}$$

is a n-dimensional matrix of parameters, where $i = 1, \ldots, p$, and p is the lag length, selected based on some information criterion; $\boldsymbol{\alpha}$ is a n-dimensional vector of parameters; finally, $\boldsymbol{\varepsilon}_t \sim iid\left(\mathbf{0}, \Sigma_\varepsilon\right)$, where Σ_ε is the residual covariance matrix.

Equation (1) can be extended to a nonlinear alternative in many different ways. For the purposes of current research, consider an additive nonlinear vector autoregression:

$$\boldsymbol{x}_t = \boldsymbol{\alpha}_0 + \sum_{i=1}^{p} B_{i,0} \boldsymbol{x}_{t-i} + \sum_{k=1}^{K} \left[\left(\boldsymbol{\alpha}_k + \sum_{i=1}^{p} B_{i,k} \boldsymbol{x}_{t-i} \right) \boldsymbol{G}\left(s_{k,t}; \boldsymbol{\theta}_k\right) \right] + \boldsymbol{\varepsilon}_t, \tag{2}$$

where K denotes the maximum number of additive regimes. $\boldsymbol{G}\left(s_{k,t}; \boldsymbol{\theta}_k\right)$ in a n-dimensional vector of transition functions, each bounded between 0 and 1. Further, $s_{k,t}$ is the regime-switching transition variable, and $\boldsymbol{\theta}_k = (\gamma_k, \boldsymbol{c}_k)$ is a set of parameters defining the shape of the transition function. Set

$K = 1$, i.e. assume a two-regime model, and consider the following representation of the transition function:

$$G(s_t; \gamma, \mathbf{c}) = \left\{1 + \exp\left[-\gamma_m / \sigma_{s_t}^m \prod_m (s_t - c_m)^m\right]\right\}^{-1} \tag{3}$$

where σ_{s_t} is the standard deviation of the transition variable. By setting $m = 1$ we obtain the so called *logistic* transition function, which has been most frequently applied in the smooth transition modelling literature (e.g. Weise, 1999; Rothman et al., 2001; Camacho, 2004).

For convenience, let's disentangle the weakly exogenous equation from the system of endogenous equations, and rewrite equation (1) as follows:

$$\boldsymbol{y}_t = \tilde{\boldsymbol{\alpha}} + \sum_{i=1}^{p} \tilde{B}_i \boldsymbol{y}_{t-i} + \sum_{i=1}^{p} \tilde{\boldsymbol{\beta}}_i z_{t-i} + \boldsymbol{\upsilon}_t \tag{4}$$

$$z_t = \alpha + \sum_{i=1}^{p} \beta_i z_{t-i} + \nu_t \tag{5}$$

where $\tilde{\boldsymbol{\alpha}}$ and $\tilde{B}_i$ are $n-1$-dimensional vector and matrices, respectively, and $\tilde{\boldsymbol{\beta}}_i = (\beta_{y_1,i}^z, \ldots, \beta_{y_{n-1},i}^z)'$. A smooth transition version of these models, with $K = 1$, is then given by:

$$\begin{aligned} \boldsymbol{y}_t = {} & \tilde{\boldsymbol{\alpha}}_0 + \sum_{i=1}^{p} \tilde{B}_{i,0} \boldsymbol{y}_{t-i} + \sum_{i=1}^{p} \tilde{\boldsymbol{\beta}}_{i,0} z_{t-i} \\ & + \left(\tilde{\boldsymbol{\alpha}}_1 + \sum_{i=1}^{p} \tilde{B}_{i,1} \boldsymbol{y}_{t-i} + \sum_{i=1}^{p} \tilde{\boldsymbol{\beta}}_{i,1} z_{t-i}\right) \tilde{\boldsymbol{G}}(s_{y,t}; \boldsymbol{\theta}_y) + \boldsymbol{\upsilon}_t \end{aligned} \tag{6}$$

$$z_t = \alpha_0 + \sum_{i=1}^{p} \beta_{i,0} z_{t-i} + \left(\alpha_1 + \sum_{i=1}^{p} \beta_{i,1} z_{t-i}\right) G(s_{z,t}; \boldsymbol{\theta}_z) + \nu_t \tag{7}$$

where, moreover, $\tilde{\boldsymbol{G}}(s_{y,t}; \boldsymbol{\theta}_y) = \boldsymbol{\iota} G(s_{y,t}; \boldsymbol{\theta}_y)$, where $\boldsymbol{\iota}$ is an unit vector restricting the transition function to be common across the equations.

Whether or not STAR-type nonlinearity is an adequate feature of the data-generating process, is a hypothesis to be tested. A conventional approach with the standard test statistics, however, cannot be employed, due to the so called Davies' problem (e.g. Davies, 1977, 1987). For example, consider equation (7) in conjunction with equation (3): the nonlinear STAR(p) will reduce to the linear AR(p) either by imposing $\gamma = 0$ or by imposing $\alpha_1 = \beta_{1,1} = \ldots = \beta_{p,1} = 0$. Thus, γ is an unidentified nuisance parameter. Luukkonen et al. (1988) proposed a solution to the problem by approximating the transition function using Taylor series expansion. This, in turn, results in an auxiliary equation:

$$z_t = \varphi_0 + \sum_{j=0}^{3}\sum_{i=1}^{p} \varphi_{i,j} z_{t-i} s_t^j + \xi_t \tag{8}$$

where ξ_t combines the original error term, ν_t, and the approximation error resulted from the Taylor series expansion. Conventional testing methods can now be applied to equation (8) to test for linearity against the STAR specification. In particular, the test is equivalent to testing the null hypothesis of H_0': $\varphi_{i,1} = \varphi_{i,2} = \varphi_{i,3} = 0$, $i = 1, \ldots, p$.

Similar approach can be applied to test linearity in a multivariate setting (e.g. Camacho, 2004). In particular, consider the system of auxiliary equations:

$$\boldsymbol{y}_t = \boldsymbol{\phi}_0 + \sum_{j=0}^{3}\sum_{i=1}^{p} \Phi_{i,j} \boldsymbol{y}_{t-i} \boldsymbol{s}_t^j + \sum_{j=0}^{3}\sum_{i=1}^{p} \boldsymbol{\phi}_{i,j} z_{t-i} \boldsymbol{s}_t^j + \boldsymbol{\zeta}_t \tag{9}$$

The nonlinearity test is equivalent to a system-wide test of $\Phi_{i,1} = \Phi_{i,2} = \Phi_{i,3} = \mathbf{0}$ and $\boldsymbol{\phi}_{i,1} = \boldsymbol{\phi}_{i,2} = \boldsymbol{\phi}_{i,3} = \mathbf{0}$, $i = 1, \ldots, p$. In small samples the higher order polynomial terms can be ignored (e.g. Weise, 1999), yielding the more "manageable" version of the system of auxiliary equations:

$$\boldsymbol{y}_t = \boldsymbol{\phi}_0 + \sum_{i=1}^{p} \Phi_{i,0} \boldsymbol{y}_{t-i} + \sum_{i=1}^{p} \boldsymbol{\phi}_{i,0} z_{t-i} + \sum_{i=1}^{p} \Phi_{i,1} \boldsymbol{y}_{t-i} \boldsymbol{s}_t + \sum_{i=1}^{p} \boldsymbol{\phi}_{i,1} z_{t-i} \boldsymbol{s}_t + \boldsymbol{\zeta}_t \tag{10}$$

where the test is equivalent of testing the null hypothesis of H_0'': $\Phi_{i,1} = \boldsymbol{\phi}_{i,1} = \mathbf{0}$, $i = 1, \ldots, p$.

3 Data

This study applies monthly data obtained from the National Oceanic and Atmospheric Administration and the International Grains Council (see Figure 1). It uses the *Niño3.4* anomaly index as a proxy for the ENSO anomalies. The *Niño3.4* series are collected from the National Oceanic and Atmospheric Administration's Climate Prediction Center.[2] The index is derived from daily sea-surface temperature values interpolated from weekly measures obtained from both satellites and actual locations around the Pacific. The sea-surface temperature anomaly in a given month, then, is the deviation in that particular month from the average historic *Niño 3.4* measure relative to the 1981 – 2010 base period.

The wheat price series are from the Argentinian, Australian, Canadian, EU, and U.S. markets. Several observations were missing from the raw data. The missing observations were interpolated by regressing the series of interest on the nearby futures prices of the soft red winter wheat as quoted on the Chicago Board of Trade, while controlling for the seasonal component. The nominal prices

[2]Available online at http://www.cpc.ncep.noaa.gov/data/indices/sstoi.indices.

were adjusted to the 2010 levels using U.S. Producer Price Index for all commodities, obtained from the U.S. Bureau of Labor Statistics. Finally, the real price series were transformed to natural logarithms, to mitigate potential heteroskedasticity in the series, to facilitate the interpretation of the impulse-responses in percentage terms, and to avoid any inadequate negative realization of the prices in the out-of-sample simulation analysis.

4 Model Selection, Estimation, and Interpretation

Following Brunner (2002), ENSO is assumed weakly exogenous to wheat prices. As such, $z_t = f(z_{t-1}, z_{t-2}, \ldots)$ and $\boldsymbol{y}_t = g(\boldsymbol{y}_{t-1}, \boldsymbol{y}_{t-2}, \ldots, z_t, z_{t-1}, \ldots)$ are considered, where z_t denotes the sea-surface temperature anomaly at time t, and $\boldsymbol{y}_t = (p_t^{\mathrm{USA}}, p_t^{\mathrm{CAN}}, p_t^{\mathrm{AUS}}, p_t^{\mathrm{FRA}}, p_t^{\mathrm{ARG}})'$ is a vector of wheat prices. The $f(\cdot)$ and $g(\cdot)$ may be nonlinear functions.

The algorithm of model selection is as follows. First, the autoregressive lag length is determined, based on multivariate Bayesian Information Criterion (BIC), subject to no residual autocorrelation. Then the models are tested against the null of linearity, using the auxiliary regressions given by equations (8) and (10). The STAR and VSTAR models are then estimated, using lagged ENSO anomaly as a transition variable. The estimated models are then tested for no remaining nonlinearity, structural change, or residual autocorrelation.

Based on BIC, and subject to no residual autocorrelation, the autoregressive order was set to three. Additionally, monthly binary variables were also included in the regressions to account for a possible seasonality in the data. The selected (autoregressive) structure of linear models are carried over in testing and estimation of the nonlinear alternatives.

The candidate transition variables were lags of ENSO, z_{t-d}, where $0 < d \leq p$ in the case of ENSO equation, and $0 \leq d \leq p$ in the case of the system of price equations. Eventually, we estimated the following nonlinear models:

$$\begin{aligned}\boldsymbol{y}_t = {}& \tilde{\boldsymbol{\alpha}}_0 + \sum_{i=1}^{p} \tilde{B}_{i,0}\boldsymbol{y}_{t-i} + \sum_{i=1}^{p} \tilde{\boldsymbol{\beta}}_{i,0} z_{t-i} + \Pi_0 \boldsymbol{D}_t \\ & + \left(\tilde{\boldsymbol{\alpha}}_1 + \sum_{i=1}^{p} \tilde{B}_{i,1}\boldsymbol{y}_{t-i} + \sum_{i=1}^{p} \tilde{\boldsymbol{\beta}}_{i,1} z_{t-i} + \Pi_1 \boldsymbol{D}_t\right) \boldsymbol{\iota} G\left(s_{y,t}, \gamma_y, c_y\right) + \boldsymbol{\upsilon}_t\end{aligned} \tag{11}$$

$$z_t = \alpha_0 + \sum_{i=1}^{p} \beta_{i,0} z_{t-i} + \pi_0' \boldsymbol{D}_t + \left(\alpha_1 + \sum_{i=1}^{p} \beta_{i,1} z_{t-i} + \pi_1' \boldsymbol{D}_t\right) G\left(s_{z,t}; \gamma_z, c_z\right) + \nu_t \tag{12}$$

where $s_{y,t} = z_t$ and $s_{z,t} = z_{t-3}$ are the selected transition variables. The estimated transition functions are:

$$G\left(s_{y,t}, \hat{\gamma}_y, \hat{c}_y\right) = \left\{1 + \exp\left[-\underset{(-)}{9.10}/\sigma_{s_{y,t}}\left(z_t + \underset{(-)}{0.99}\right)\right]\right\}^{-1} \tag{13}$$

and

$$G\left(s_{z,t}; \hat{\gamma}_z, \hat{c}_z\right) = \left\{1 + \exp\left[-\underset{(1.96)}{4.62}/\sigma_{s_{z,t}}\left(z_{t-3} - \underset{(0.10)}{0.02}\right)\right]\right\}^{-1} \tag{14}$$

The values in parentheses are asymptotic standard errors of the parameter estimates. In the case of price equations, the gridsearch routine was implemented to approximate the nonlinear least squares estimation of the VSTAR model. The approach, in principle, is similar to the so called SlowShift algorithm suggested by Enders and Holt (2011), who note that "with fine enough grid the in-sample mean square prediction error will be effectively minimized". These estimated functions are presented in Figures 2 and 3. In both instances the smooth transition between the regimes is apparent. In the case of ENSO, the inflection point of the transition function is centered around zero, as such, the autoregressive dynamics differ between El Niño and La Niña regimes. In the case of the system of price equations, the estimated function identifies the "extreme" La Niña regime with distinct price dynamics, as compared to the "other" regime.

There are a number of ways to examine the dynamics of the estimated models. This study adopts the generalized impulse–response (GIR) functions of Koop et al. (1996) for this purpose. The method is imperative when dealing with nonlinear models, which are not invariant to the information set prior the shocks, the sign and magnitude of the shocks, as well as, the idiosyncratic disturbances that occur throughout the forecast horizon. Thus, a GIR at a horizon h, for a given shock ν_t, and a history ω_{t-1}, is defined as:

$$\text{GIR}\left(h, \nu_t, \omega_{t-1}\right) = E\left(y_{t+h}|\nu_t, \omega_{t-1}\right) - E\left(y_{t+h}|\omega_{t-1}\right) \tag{15}$$

Thus, GIR is a function of ν_t and ω_{t-1}, which, in turn, are realizations of random variables V_t and Ω_{t-1}. Therefore, GIR can also be given as a realization of a random variable:

$$\text{GIR}\left(h, V_t, \Omega_{t-1}\right) = E\left(y_{t+h}|V_t, \Omega_{t-1}\right) - E\left(y_{t+h}|\Omega_{t-1}\right) \tag{16}$$

In the current exercise, we follow the simulation algorithm similar to Skalin and Teräsvirta (2002). We randomly sample (without replacement) 100 histories as starting points for the GIR analysis. We sample 50 random shocks from the pool of residuals of the estimated model, and for each history-shock combination compute 500 bootstrap vectors of length equal to 36 months. This way, a sufficiently large number of extrapolated sequences are obtained to approximate the densities at each horizon. We also incorporate idiosyncratic innovations from the pool of residuals of the estimated models. The extrapolated series from ENSO equation are then embedded in the system of price equations, to obtain GIRs for wheat prices, using the sampling procedure similar to the aforementioned. Mean responses, i.e. GIRs, are obtained by averaging the realized extrapolated series across the bootstrap iterations for given initial shock and history. These GIRs are then averaged to illustrate the dynamics over the 36 month horizon (see Figure 4). In addition, the distributions of these GIRs, for horizons $h = 1, 4, 12, 24$, are presented in Figure 5.

Several features of interest should be noted. First of all, the El Niño shocks result in reduction of wheat prices, while the opposite effect is observed after the La Niña shocks. The magnitude and economic significance of these effects is somewhat modest, which is partly due to the offsetting effects of ENSO in different parts of the world. For example, droughts in North America are known to be associated with the La Niña phase of the phenomenon, while in Australia the similar weather effect coincides with the El Niño phase.

Another interesting feature of the observed dynamics is that the response functions to ENSO impulses are asymmetric – the GIRs after a positive shock are not mirror images of the GIRs after a negative shock. On average, prices tend to increase at a higher rate (approximately one-to-two percentage points more, which translates to roughly 50-80 percent difference) after the La Niña shocks, as compared to their decrease after the El Niño shocks.

Finally, as the horizon length grows, the distributions of the GIRs converge to "spikes" at 0, which is illustrative of the time series processes being stationary and ergodic (Dijk et al., 2000).

5 Conclusion

This study examines ENSO-induced asymmetries in the international wheat price dynamics. Using the three decades of monthly data and smooth transition modelling methodology, the outcome of this research suggests that there are indeed STAR-type nonlinearities in ENSO cycles as well as in the vector of wheat price series. Moreover, wheat prices tend to respond to ENSO shocks in the short- and intermediate-run horizons. In particular, the study finds that a positive ENSO shock, i.e. El Niño, results in decreased wheat prices, while a negative ENSO shock, i.e. La Niña, results in increased wheat prices. The price changes vary across the regions of export origin, but are all within five percent magnitude. More interestingly, the price responses to ENSO shocks are asymmetric – the La Niña effect is (in absolute terms) larger as compared to the El Niño effect.

This analysis contributes to the growing literature in economics of climate anomalies. It quantifies a rather trivial link between supply shocks due to ENSO anomalies, and the subsequent wheat price fluctuations. This research will interest researchers in the fields of time series econometrics, price analysis, and climate economics. Moreover, because wheat is one of the most exported grains and main staples around the world, this research also offers implications for international trade and economic development.

References

Bessler, D. A., J. Yang, and M. Wongcharupan (2003). Price Dynamics in the International Wheat Market: Modeling with Error Correction and Directed Acyclic Graphs. *Journal of Regional Science 43*(1), 1–33.

Brunner, A. (2002). El Nino and World Primary Commodity Prices: Warm Water or Hot Air? *Review of Economics and Statistics 84*(1), 176–183.

Camacho, M. (2004). Vector Smooth Transition Regression Models for US GDP and the Composite Index of Leading Indicators. *Journal of Forecasting 23*(3), 173–196.

Cashin, P., C. J. McDermott, and A. Scott (2002). Booms and Slumps in World Commodity Prices. *Journal of Development Economics 69*(1), 277–296.

Davies, R. (1977). Hypothesis Testing when a Nuisance Parameter is Present only under the Alternative. *Biometrika 64*(2), 247–254.

Davies, R. (1987). Hypothesis Testing when a Nuisance Parameter is Present only under the Alternative. *Biometrika 74*(1), 33–43.

Dijk, D. J. C., P. H. Franses, and H. P. Boswijk (2000). Asymmetric and Common Absorption of Shocks in Nonlinear Autoregressive Models. Technical report, Econometric Institute Research Papers.

Enders, W. and M. T. Holt (2011). Breaks, Bubbles, Booms, and Busts: The Evolution of Primary Commodity Price Fundamentals. MPRA Paper No. 31461.

Goodwin, B. K. and N. E. Piggott (2001). Spatial Market Integration in the Presence of Threshold Effects. *American Journal of Agricultural Economics 83*(2), 302–317.

Goodwin, B. K. and T. C. Schroeder (1991). Price Dynamics in International Wheat Markets. *Canadian Journal of Agricultural Economics 39*(2), 237–254.

Koop, G., M. Pesaran, and S. Potter (1996). Impulse Response Analysis in Nonlinear Multivariate Models. *Journal of Econometrics 74*(1), 119–147.

Luukkonen, R., P. Saikkonen, and T. Teräsvirta (1988). Testing Linearity Against Smooth Transition Autoregressive Models. *Biometrika 75*(3), 491–499.

Mallya, G., L. Zhao, X. Song, D. Niyogi, and R. Govindaraju (2013). 2012 Midwest Drought in the United States. *Journal of Hydrologic Engineering 18*(7), 737–745.

Mohanty, S., W. H. Meyers, and D. B. Smith (1999). A Reexamination of Price Dynamics in the International Wheat Market. *Canadian Journal of Agricultural Economics 47*(1), 21–29.

Mohanty, S., E. W. F. Peterson, and N. C. Kruse (1995). Price Asymmetry in the International Wheat Market. *Canadian Journal of Agricultural Economics 43*(3), 355–366.

Ropelewski, C. and M. Halpert (1987). Global and Regional Scale Precipitation Patterns Associated with the El Niño/Southern Oscillation. *Monthly Weather Review 115*(8), 1606–1626.

Rosenzweig, C., A. Iglesias, X. Yang, P. R. Epstein, and E. Chivian (2001). Climate Change and Extreme Weather Events: Implications for Food Production, Plant Diseases, and Pests. *Global Change & Human Health 2*(2), 90–104.

Rothman, P., D. van Dijk, and P. H. Franses (2001). Multivariate STAR Analysis of Money–Output Relationship. *Macroeconomic Dynamics 5*(4), 506–532.

Skalin, J. and T. Teräsvirta (2002). Modeling Asymmetries and Moving Equilibria in Unemployment Rates. *Macroeconomic Dynamics 6*(2), 202–241.

Teräsvirta, T. (1994). Specification, Estimation, and Evaluation of Smooth Transition Autoregressive Models. *Journal of the American Statistical Association 89*(425), 208–218.

Tong, H. (1990). *Non-linear Time Series: A Dynamical System Approach.* Oxford University Press.

Tong, H. and K. S. Lim (1980). Threshold Autoregression, Limit Cycles and Cyclical Data. *Journal of the Royal Statistical Society. Series B (Methodological) 42*(3), 245–292.

van Dijk, D., T. Teräsvirta, and P. Franses (2002). Smooth Transition Autoregressive Models – A Survey of Recent Developments. *Econometric Reviews 21*(1), 1–47.

Weise, C. (1999). The Asymmetric Effects of Monetary Policy: A Nonlinear Vector Autoregression Approach. *Journal of Money Credit and Banking 31*(1), 85–108.

Figures

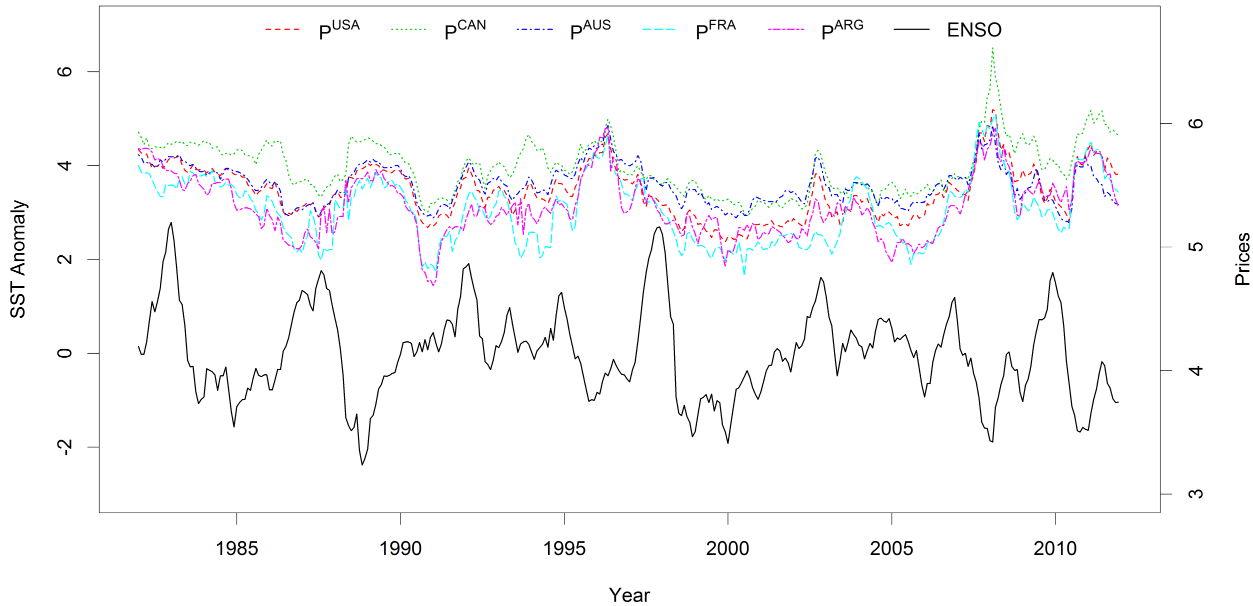

Note: the prices are natural logarithms of the real wheat prices denominated in 2010 $US.

Figure 1: Monthly Series of ENSO and Wheat Prices

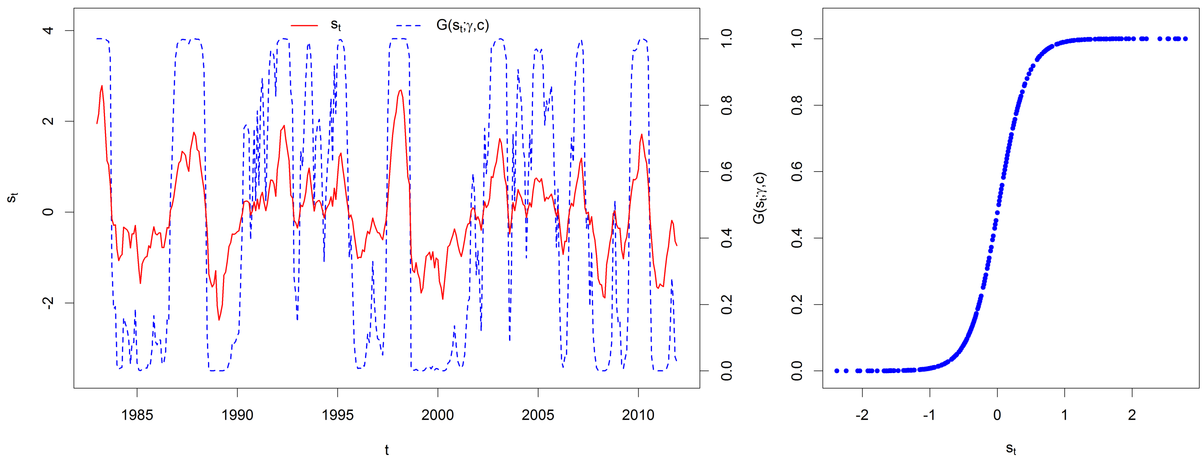

Figure 2: The Estimated Transition Function for ENSO

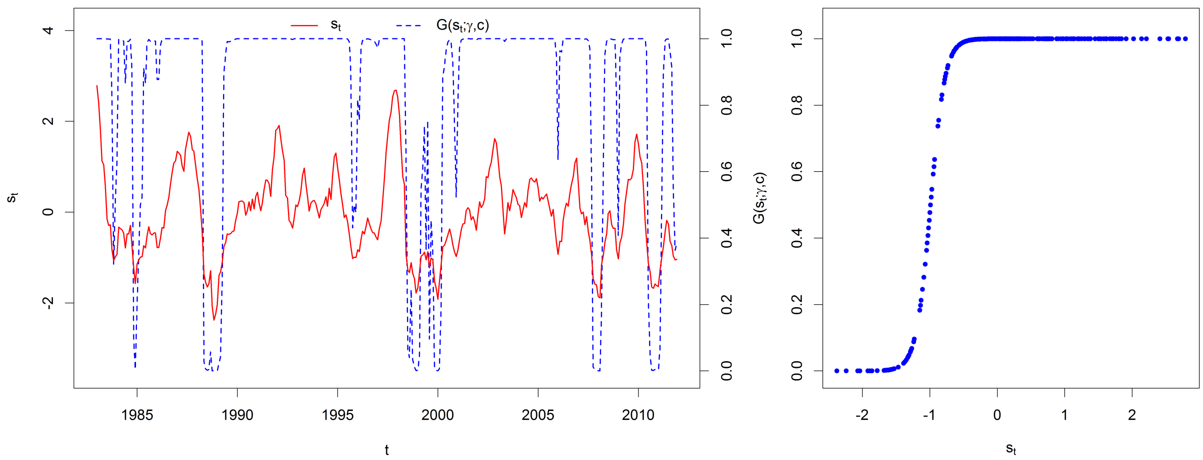

Figure 3: The Estimated Transition Function for Wheat Prices

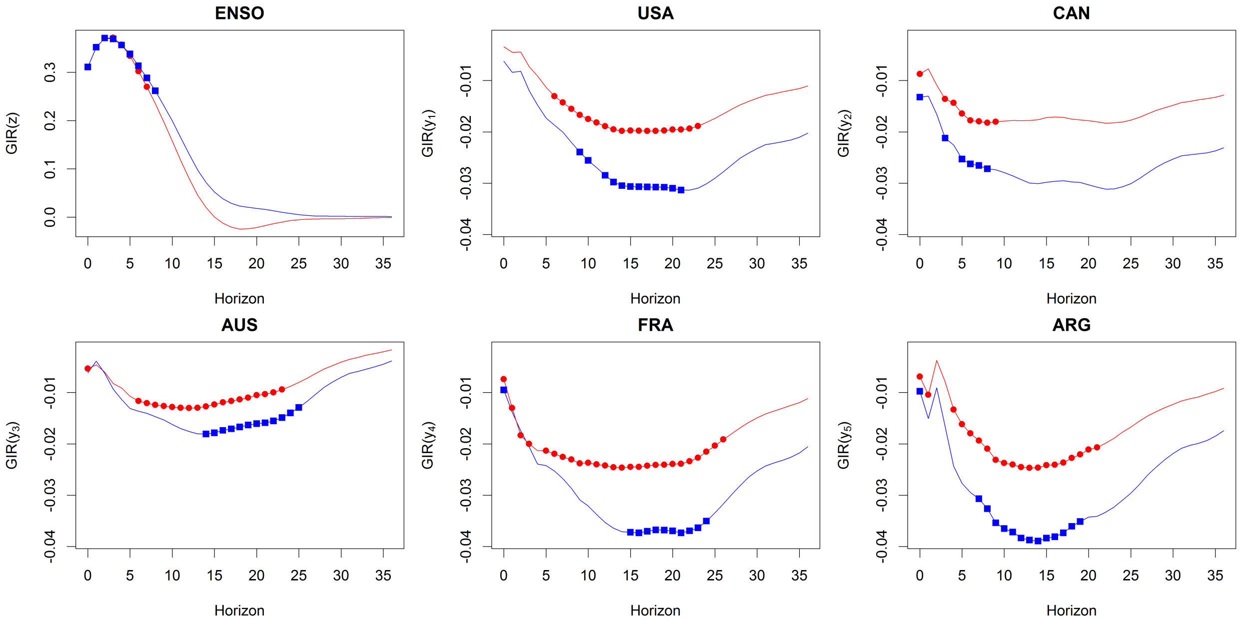

Note: GIRs in red are associated with the El Niño shocks, and GIRs in blue are associated with the La Niña shocks. Additionally, GIRs associated with the La Niña shocks are multiplied by negative one, and thus inverted, to facilitate the comparison with the analogous (but opposite in sign) El Niño shocks.

Figure 4: Generalized Impulse–Response Extrapolates

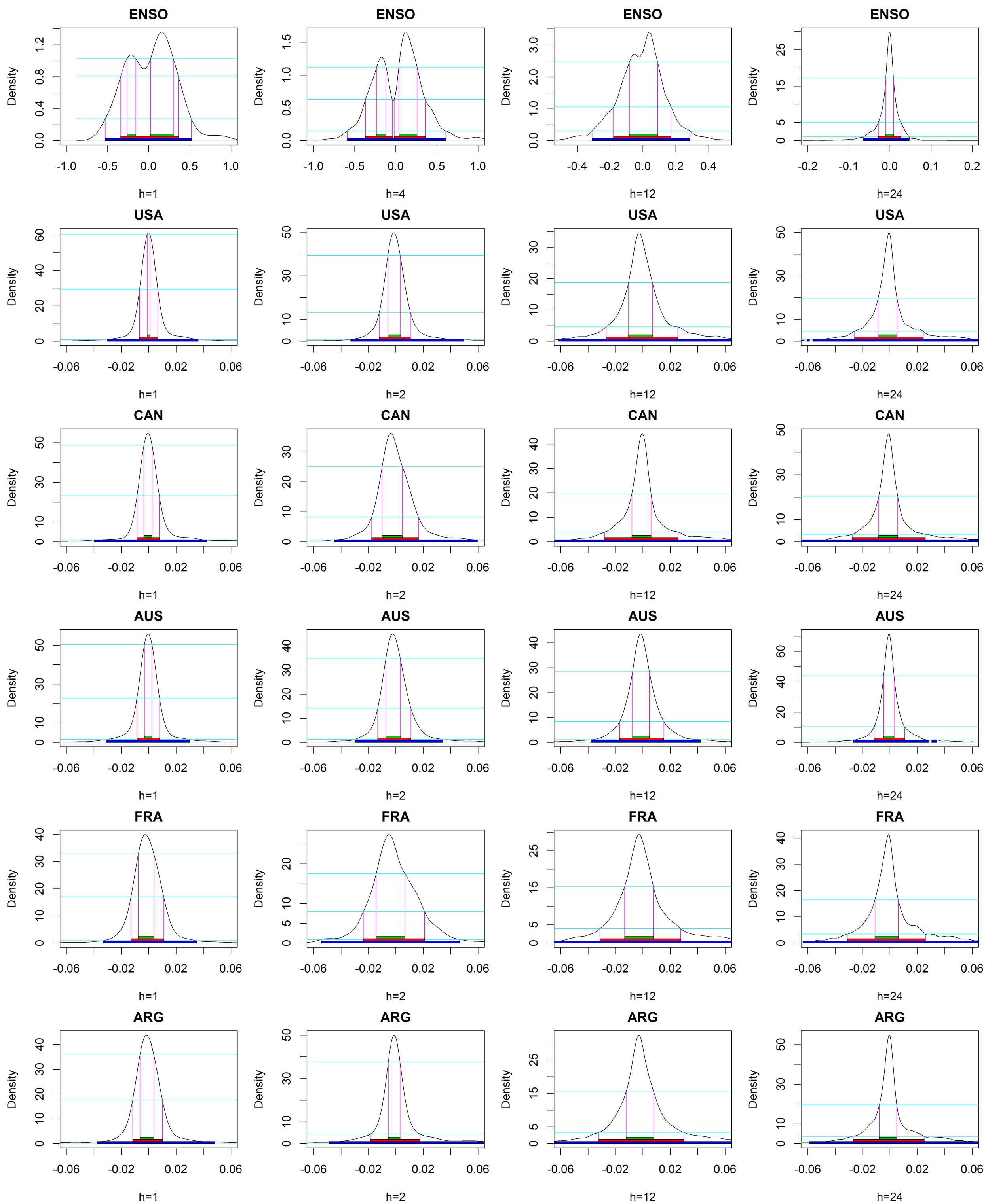

Figure 5: Generalized Impulse–Response Densities